POLITECNICO DI TORINO
Repository ISTITUZIONALE

3D FDM production and mechanical behavior of polymeric sandwich specimens embedding classical and honeycomb cores.

(Article begins on next page)

18 April 2024

Research Article

Salvatore Brischetto*, Carlo Giovanni Ferro, Roberto Torre, and Paolo Maggiore

3D FDM production and mechanical behavior of polymeric sandwich specimens embedding classical and honeycomb cores

Abstract: Desktop 3D FDM (Fused Deposition Modelling) printers are usually employed for the production of non-structural objects. In recent years, the present authors tried to use this technology also to produce structural elements employed in the construction of small UAVs (Unmanned Aerial Vehicles). Mechanical stresses are not excessive for small multirotor UAVs. Therefore, the FDM technique combined with polymers, such as the ABS (Acrylonitrile Butadiene Styrene) and the PLA (PolyLactic Acid), can be successfully employed to produce structural components. The present new work is devoted to the production and preliminary structural analysis of sandwich configurations. These new lamination schemes could lead to an important weight reduction without significant decreases of mechanical properties. Therefore, it could be possible, for the designed application (e.g., a multifunctional small UAV produced via FDM), to have stiffener and lighter structures easy to be manufactured with a low-cost 3D printer. The new sandwich specimens here proposed are PLA sandwich specimens embedding a PLA honeycomb core produced by means of the same extruder, multilayered specimens with ABS external layers and an internal homogeneous PLA core using different extruders for the two materials, sandwich specimens with external ABS skins and an internal PLA honeycomb core using different extruders for the two materials, and sandwich specimens where two different extruders have been employed for PLA material used for skins and for the internal honeycomb core. For all the proposed configurations, a de-tailed description of the production activity is given. Moreover, several preliminary results about three-point bending tests, different mechanical behaviors and relative delamination problems for each sandwich configuration will be discussed in depth.

Keywords: Fused Deposition Modelling (FDM); 3D printing process; additive manufacturing; sandwich structures; honeycomb core; ABS material; PLA material; bending tests

1 Introduction

Additive Manufacturing (AM) processes usually generate layered parts. These technologies are not exclusively used for prototyping any longer. New AM opportunities and applications recently appeared in the literature even though the economical impact is still modest. A possible AM technology classification was proposed by Levy et al. [1] where the development years were given in brackets. This partial list was: Stereolithography - SLA (1986-1988), Solid Ground Curing - SGC (1986-1988), Laminated Object Manufacturing - LOM (1985-1991), Fused Deposition Modelling - FDM (1988-1991), Selective Laser Sintering - SLS (1987-1992) and 3D Printing (Drop on Bed) - 3DP (1985-1997). Additive Manufacturing (AM) was first patented in 1984 by the French scientist Alain Le Mehaute. Its distinctive feature is the addition of material with different methods (e.g., powder or wire) in place of the subtraction of material from a raw part. AM was widely introduced in the preliminary and conceptual design phase thanks to its reduced production costs and realization time for a prototype. In the last two decades, this technique was also considered for low-scale mass production [2]. 3D printing will propel the revolution of fabrication modes forward, and bring in a new era for customized fabrication by means of the five *any* [3]: use of almost *any* material to fabricate *any* part, in *any* quantity and *any* location, for *any* industrial field. Innovations in material, design and fabrication pro-

*Corresponding Author: Salvatore Brischetto: Department of Mechanical and Aerospace Engineering, Politecnico di Torino, corso Duca degli Abruzzi, 24, 10129 Torino, Italy; Email: salvatore.brischetto@polito.it, Tel: +39.011.090.6813, Fax: +39.011.090.6899

Carlo Giovanni Ferro, Roberto Torre, Paolo Maggiore: Department of Mechanical and Aerospace Engineering, Politecnico di Torino, Turin, Italy

cesses will be inspired by the merging of 3D-printing technologies and processes with respect to traditional manufacturing processes. Finally, for manufacturing industries, 3D printing will become as valuable as subtractive manufacturing processes. The AM process extensively employed in the present work will be the Fused Deposition Modelling (FDM) technology because of its simplicity and low costs. The present authors showed in [4] an innovative multirotor Unmanned Aerial Vehicle (UAV) which was able to easily and quickly change its configuration. The proposed multi-rotor system was inexpensive because of the few universal pieces needed to compose the platform which allowed the creation of a kit (see the patent application [5]). This modular kit allowed to have a modular drone with different configurations. Such configurations were distinguished among them for the number of arms, number of legs, number of rotors and motors, and landing capability. Another innovation feature was the introduction of the 3D printing technology to produce all the structural elements. In this way, all the pieces were designed to be produced via the Fused Deposition Modelling (FDM) technology using desktop 3D printers and polymeric materials. Therefore, an universal, dynamic and economic multi-rotor UAV was developed and called PoliDrone. One of the most important target of the PoliDrone project is to have a total weight (comprising the pay-load) always less than 2 kilos for each possible configuration. A possibility to reduce such a weight could be the use of sandwich parts in polymeric materials and produced via the FDM technology. This target justifies the developing of this new paper. The main improvements in future aircraft and spacecraft may depend on an increasing use of conventional and unconventional multilayered structures [6]. One of these advanced configurations are the sandwich structures with honeycomb or metallic foams used as core-layers which are lightweight with high bending stiffness. Goh et al. [7] proposed the use of sandwich structures produced via AM technology in light-weight UAVs in order to have better performance in terms of shorter take-off range and longer flight endurance. However, light-weight structures with complex inner parts are hard to be produced using conventional manufacturing methods. The ability to print directly complex inner structures without the need of a mould gives additive manufacturing (AM) an edge over conventional manufacturing. Recent developments in composite and multi-material printing open up new possibilities of printing light-weight structures and novel platforms like flapping wings with ease. However, the successfully application of the FDM technology in the production of small structural elements, and in particular sandwich structures, requires a depth material character-

ization and systematic and rigorous mechanical behavior analyses as stated in [8].

Typical sandwich structures produced via classical manufacturing processes are very common in the open literature. The flexural behavior of sandwich structures was usually experimentally determined by means of three- or four-point bending tests [9]. The typical skin-core delamination failure was influenced by eventual stresses orthogonal to the middle plane of the sandwich and it was due to the low shear stiffness and the elastic constant mismatches of the skins and core material [10]. The skin-core delaminations in classical sandwich structures were extensively described in [11] and [12]. In sandwich structures produced via FDM technology, the already mentioned problems, related to classical sandwich configurations discussed in [9–12], are in addition to the typical problems connected with structural elements produced via FDM [13–16]. Luzanin et al. [13] proposed three-point bending tests for homogeneous specimens made of PLA. The proposed experimental analysis was influenced by the layer thickness, deposition angle and infill percentage. All these parameters had influence on the maximum flexural force in FDM specimens made of PolyLactic Acid (PLA). Melnikova et al. [14] described the effects of different materials (in particular Acrylonitrile Butadiene Styrene (ABS) and PLA) in the FDM technique used for the production of structural elements. Gu and Li [15] used the fused deposition modelling process in the construction of elements for biomedical structures having complex geometry. The manufacturing parameters of deposition orientation and density were modeled for fabrication of prototypes with functionally graded properties. The manufacturing efficiency of the FDM technologies was investigated in [16] where the filling rate was analyzed in order to reduce the filament consumption. Interesting ideas about production activity and experimental mechanical analysis of composite and sandwich specimens produced via FDM technology can be found in [17–35]. FDM composite elements were described and analyzed in [17–25]. FDM sandwich structures are the topic of works [26–35] with particular attention to classical homogeneous cores in [26–28], honeycomb cores in [29–31] and auxetic cellular structures and lattice materials in [32–35]. Minetola et al. [17] proposed the use of a filament made of a Polyammide (PA) blend as a reinforcement in multimaterial PLA beams produced via FDM. The flexural behaviour of these composite beams was evaluated by means of three-point bending tests. Experimental results were compared with those of the finite element simulations, and the influence of the layer-by-layer fabrication on the beam resistance was also discussed. Kumar and Kruth [18] discussed the use of rapid prototyping (RP) technol-

ogy for rapid tooling and rapid manufacturing for the development of application-oriented composites. The paper proposed brief notes on the composites produced using main rapid prototyping processes such as Selective Laser Sintering/Melting, Laser Engineered Net Shaping, Laminated Object Manufacturing, Stereolithography, Fused Deposition Modelling, Three Dimensional Printing and Ultrasonic Consolidation. Specimens with different raster orientations for each layer (sandwich-like configurations) were built in [19] via FDM technology. The final stiffness and strength of the specimens were determined in tensile and bending tests, and the stiffness was predicted using classical lamination theory. Parandoush and Lin [20] proposed an interesting review paper about different AM technologies for the production of composite elements with polymeric matrices reinforced with different fibre types. Although AM for fiber/polymer composites is increasing, there are some issues which must be addressed including void formation, poor adhesion of fibers and matrix, blockage due to filler inclusion, increased curing time, modelling, simulation, and so on. For these reasons, AM capabilities must be further enhanced by incorporating multiple materials in its processes as discussed in [21]. Es-Said et al. [22] proposed the study of tensile strength, modulus of rupture and impact resistance for different layer orientations of ABS rapid prototype solid models. The samples were fabricated by a Stratasys rapid prototyping machine in five different layer orientations. The 0° orientation, where layers were deposited along the length of the samples, displayed superior strength and impact resistance over all the other orientations. The anisotropic properties were probably caused by weak interlayer bonding and interlayer porosity. The mechanical properties of parts produced via FDM are strictly connected with significant voids between deposition lines. In the study proposed in [23], a novel approach, that adding thermally expandable microspheres into matrix and combining FDM process with thermal treatment, was proposed to contrast this problem. The influences of microsphere content, heating temperature and heating time were investigated. Bade et al. [24] discussed the possible applications of AM methods for the production of Carbon Fibre (CF) components without the aid of mould or plug used by traditional methods. They investigated the possible AM designing techniques to experimentally prove the validity of the research to develop a design concept which could be embedded into an AM machine as a 3D Printer. PolyLactic Acid (PLA) tensile test specimens were produced with Carbon Fibre (CF) reinforcements using both traditional moulding and AM techniques. The preliminary mechanical testing of moulded specimens with fibres revealed a tensile strength increase of up to 73% when compared to PLA specimens without fibres. Work [25] reviewed the state-of-the-art and discussed challenges connected with the use of additive manufacturing for directionally reinforced composite processings. Wiliams et al. [26] investigated the feasibility of using Rapid Prototyping (RP) technologies (Stereolithography (SLA), Fused Deposition Modelling (FDM), and Three-Dimensional Printing (3DP)) for fabrication of the core of a composite sandwich structure. Control cores of a flat geometry were fabricated from epoxy using SLA and from ABS plastic using FDM. Corrugated geometry cores were fabricated using SLA, FDM and 3DP. Carbon-epoxy composite sandwich structures were fabricated from all cores using a wet-hand lay-up process with vacuum cure. The performance of each core was measured using a bending test to determine bending stiffness and failure load. Composite sandwich structures with corrugated ABS plastic cores outperformed those with flat ABS plastic cores. Several manufacturing demonstrations were performed in [27] including the fabrication of a discrete PC-ABS sandwich structure containing tetragonal truss core elements. The crack initiation and crack propagation of 3D printed corrugated sandwich structures, using acoustic emission technique, were investigated in [28]. Vertical pillars were introduced between the existing sinusoidal-wave-like corrugations to improve the load bearing capacity of these structures. Bagsik et al. [29] analyzed the mechanical behavior of lightweight parts manufactured with the 3D production system Fortus 400mc and the material Polyetherimide (PEI). The test specimens were built up with different inner structures and building directions. Therefore, test specimens with known lightweight core geometries (e.g., corrugated and honeycomb cores) were designed. A four-point bending test was conducted to analyze the strength properties as well as the weight-related strength properties. The influence of the structure width, the structure wall thickness and the top layer thickness was analyzed in honeycomb structures. Li and Wang [30] combined 3D printing technique, numerical analysis and experiments to design a new class of sandwich composites that exhibit various bending behaviors. These programmed sandwich structures contained 3D printed core materials with truss, conventional honeycomb and re-entrant honeycomb topologies. Three-point bending tests were performed to investigate the bending behavior of these sandwich composites with two types of carbon fiber reinforced polymer face sheets. A detailed description for the construction of sandwich structures with honeycomb core produced via Additive Layer Manufacturing (ALM) process was given in [31]. The proposed approach allowed a reduction for the mass of sandwich components of about 50% if compared

to conventional approaches. An analytical model of a 3D re-entrant honeycomb auxetic cellular structure was established in [32] using a large deflection Timoshenko beam model. Analytical solutions for the elastic modulus, Poisson ratio and yield strength of the cellular structure in all principal directions were obtained, they indicated a wide range of mechanical property control via geometrical designs. The results were compared with experimental tests and finite element analyses. Lattice materials could satisfy the need of light and stiff structures in the aerospace industry. For example, the wing leading edge is one of the most critical part for both on-board subsystem and structural elements. Nowadays, this part is made by different components bonded together such as external skins, internal passageways, and feeding tubes. In work [33], a single-piece multifunctional panel produced via additive manufacturing was developed. Optimal design and manufacturing were discussed according to technological constraints, aeronautical performances and sustainability. Selective Laser Melting (SLM) technology was employed for the production of this multifunctional panel. In particular, in works [34] and [35], the mechanical behaviour of this porous core sandwich was investigated by means of a comparison between results collected from experimental characterization and numerical analysis based on a dedicated finite element model.

In past authors' works, homogeneous polymeric specimens were tested and capability and statistical analyses were performed. Tensile tests for homogeneous specimens made of ABS were conducted in [36]. Geometrical and mechanical properties of produced specimens, such as tensile strength and stiffness, were evaluated. ASTM 638 type specimens were used. A capability analysis was applied for both mechanical and dimensional performances. Statistically stable limits were determined using experimentally collected data. Brischetto et al. [37] proposed a statistical characterization of the mechanical properties of ABS specimens in compression tests in analogy with work [36] about the tensile characterization of ABS specimens. A desktop 3D printer, including ABS filaments as material, was employed. ASTM 625 standard was considered as the reference normative. A capability analysis was also used as a reference method to evaluate the boundaries of acceptance for both mechanical and dimensional performances. The statistical characterization and the capability analysis were proposed in an extensive form in order to validate a general method that could be used for further tests in a wider context. The main conclusions of works [36] and [37] were deeply discussed in [38] where for both tensile and compressive tests, Young Modulus, maximum stress at rupture and stress at proportional limit were determined. Works [39] and [40] were preliminary studies which will be investigated in details in the present new work. The present new paper is devoted to the production and preliminary structural analysis of sandwich configurations produced via FDM technology. These new lamination schemes could lead to an important weight reduction without significant decreases of mechanical properties. The new sandwich configurations here proposed will be sandwich specimens embedding honeycomb cores employing the same extruder for PLA skins and PLA core, sandwich specimens with ABS external skins and PLA homogeneous core using two different extruders, sandwich specimens with ABS external skins and PLA honeycomb core using two different extruders, and sandwich specimens embedding honeycomb cores employing two different extruders for PLA skins and PLA core. For all the proposed configurations, a detailed description of the production activity is given. Moreover, several preliminary results about three-point bending tests, different mechanical behaviors and relative delamination problems for each sandwich configuration will be discussed in depth. The paper is organized in a Section 2 about the detailed description of the sandwich production via FDM technology, in a Section 3 where preliminary bending test results and mechanical behavior descriptions of produced sandwich specimens will be discussed in details, and in a Section 4 about the main conclusions and the future developments of the proposed activity.

2 Sandwich production via FDM technology and test set-up

The specimens were printed using the home desktop Sharebot NG 3D printer with two active extruders. The technology behind this device is the FDM (Fused Deposition Modelling), also known as FFF (Fused Filament Fabrication). The process begins with a bundle of thermoplastic raw material in the form of a cylindrical filament. The polymer is mechanically dragged into the hot-end, melted and extruded on a heated glass bed. After the first layer has been completely printed, the bed moves downward and the nozzle drops off the second layer on the previous printed one, and so on. The distance between the extruder and the printing plane (which could be the glass bed during the first layer printing, or the previous layer during the printing of the next layers) defines the layer height. The path followed by the extruders during the printing process can be customized by the user. A certain number of peripheral beads are usually deposited; these beads closely fol-

low the external contour of the object and are useful in order to give a good surface finish to the final element. Once the contour is complete, the extruder starts to fill the interior. The pattern can be customized; it is usually chosen as a function of the shape of the piece and/or its particular geometry and potential symmetries. The layer height and the pattern are only two of the possible printing parameters that must be chosen to set the process. Several studies underlined that these parameters significantly affect the mechanical response of the printed elements [41–43], in particular for tensile and compression properties. Parameter values were set in analogy with past authors' works about tensile and compression tests of homogeneous polymeric specimens.

Build temperature. It is the temperature of the extruding nozzle, it is related to the specific employed polymer. Both PLA and ABS can be properly extruded using a certain temperature range. Following the manufacturer recommendations, a nozzle temperature equals 230°C for PLA and equals 250°C for ABS was set.

Layer height. It is the thickness of each printed layer. It is directly responsible of the surface finish of the piece, especially for those elements with non-horthogonal vertical walls. A layer thickness equals 0.1mm was chosen for the single-extruder printed parts and a value equals 0.3mm was set for the double-extruder printed elements.

Bed temperature. It is the temperature of the printing surface. Its main function is to improve the general adherence and to limit the shrinkage. Both these effects appear with the rapid cooling of the element. ABS is more sensible than PLA to these effects. A temperature of 80°C was set when ABS is in contact with the printing floor. A lower temperature (40°C) was set when PLA was the first material layer.

Perimeters. It is the number of peripheral beads which must be printed. Due to the simplicity of the involved geometries, 2 peripheral beads were chosen.

Raster orientation/angle. When a rectilinear pattern is selected for the internal infill, the angle of each deposited bead (with respect to a reference axis of the printing plane) must be chosen. For the homogeneous sections of the printed specimens, a criss-cross lamination with a stacking sequence of [45°/−45°] was chosen. The honeycomb core was printed without any internal infill because the walls of each hexagon element were really thick and therefore a single bead was sufficient.

Internal infill. It is the percentage of volume occupied by the extruded polymer. A 100% internal infill was set for the homogeneous sections of the printed specimens in order to obtain solid sections. This parameter is meaningless

in the case of the honeycomb core because of the previous explanations.

2.1 The specimens

The two reference standards for the evaluation of the flexural properties of un-reinforced and reinforced plastic materials are the ASTM D790 [44] and the ASTM D6272 [45]. Both the standards describe a method that involves the application of a load to a simply supported specimen having the form of a beam. The first test is accomplished with a three-point loading system, the second one uses a four-point loading system. The specimen rests on two supports in both cases, the load is applied by a single and centered nose in the first case [44], two symmetrically located noses are used in the second case [45]. The different configurations lead to a different location of the maximum axial fiber stress due to a different location of the maximum bending moment. In the ASTM D790 [44], it is suggested to use the ASTM D6272 [45] if the surface subjected to tensile stresses does not break or yield within the strain limit of 5.0%. Because of the aims of this preliminary evaluation, it was chosen to follow the dictates of the ASTM D790 [44], confirming its applicability thanks the generated results. Given a span of $90mm$ between the supports, a span-to-depth ratio of 18 was used. This feature leads to a thickness of $5mm$ for the specimen. In order to have an appropriate holder, the length of the specimens was set equal to $99.50mm$. All the specimens were $17.17mm$ wide.

The aim of this research activity is to assess the feasibility and possible benefits of sandwich structures produced using a simple desktop 3D printer. Sandwich beams are made by thin skins and a thick internal core in the form of a honeycomb configuration. The main idea behind this lamination scheme is that the total thickness of the structure could provide greater bending stiffness without any disadvantage in terms of weight.

The first idea is to test PLA sandwich specimens with a honeycomb core produced via a single extruder. Both the skins and the core are printed in sequence by means of the same (and only active) extruder. The 2D drawing of the proposed specimen is shown in Figure 1. The two external skins have a global thickness of $2mm$, the thickness of the honeycomb core is $3mm$. The hexagon is the fundamental cell of the honeycomb core and it is repeated across the width and the length of the specimen. Its apothem is equal to $2.5mm$ and its walls are $0.5mm$ thick. Two complete and two partial hexagons are arranged in specimens principal transverse direction in order to obtain a symmetric pattern with respect to the longitudinal direction. The

Table 1: Lamination scheme of the eight specimens. *HC* means *HoneyComb*. *HOM* means *HOMogeneous*.

Specimen	1	2	3	4	5	6	7	8
CORE MATERIAL	PLA	PLA	PLA	PLA	PLA	PLA	PLA	PLA
CORE TYPE	HC	HC	HC	HC	HC	HOM	HC	HC
SKIN MATERIAL	PLA	PLA	PLA	PLA	PLA	ABS	ABS	PLA
NUMBER OF EXTRUDERS	1	1	1	1	1	2	2	2

Table 2: Dimensional experimental data for the eight specimens.

	Dimensional experimental data								
Specimen	1	2	3	4	5	6	7	8	NOMINAL
Width[mm]	17.38	17.57	17.11	17.12	17.18	16.95	17.01	16.95	17.17
Thickness[mm]	5.36	5.46	5.29	5.32	5.28	5.43	5.48	5.35	5.00
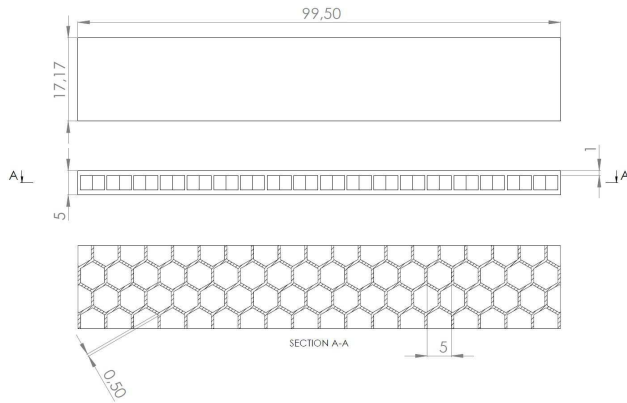
Figure 1: Nominal geometrical data of specimens 1-5, 7 and 8.

width is $17.17\,mm$. As required by the first cited standard ASTM D790 [44], 5 specimens were built and tested (specimens 1-5 in Table 1). The results were processed and the average value of the mechanical characteristics were obtained. A qualitative investigation was made in order to have valuable insights for the future developments. ABS has better mechanical characteristics than PLA. For this reason, the PLA skins have been replaced by ABS skins in specimens 6 and 7 of Table 1. As the printer has to build firstly the bottom skin, than the core and finally the top skin using different materials, this choice involves a setback. Best printing results are obtained with FDM when the deposition of the various layers is sequential and unbroken. In this way, each new layer is deposited over the old one during its solidification process. For these reasons, the filament change during the process must be avoided. Therefore, ABS and PLA are printed with a dedicated extruder for each one. The external dimensions of the specimens were the same as those considered before; at the same time the relative thickness of the lamination is kept

unaltered. The tests on these last specimens shown the performances to be significantly worse due to a limited grip between the skins and the core, but the reason is not entirely clear. The specimen 6 in Table 1 has ABS skins and a homogeneous PLA core, in order to test the adhesion from the material point of view. The specimen 7 of Table 1 is similar to specimen 6 but the internal PLA core is not homogeneous but it has a honeycomb configuration. The specimen 8 of Table 1 has PLA honeycomb core and PLA external skins, with the skins and the core separately printed with the two different extruders. In this way, it is possible to also test the adhesion from the manufacturing point of view. All these configurations are summarized in Table 1.

2.2 Test set-up

The test was carried out strictly following the procedure illustrated in ASTM D790 standard [44]. The thickness and the width of each specimen was measured, the collected results are necessary to test the process performances and to have the geometrical characteristics for the calculation of the mechanical properties. These geometrical data are given in Table 2. It is necessary to underline that a comparison cannot be done for the whole group of specimens because different sandwich configurations are considered. The nominal value for the thickness is $5\,mm$, each specimen experimented an upward deviation. The first five specimens are comparable because they use the same sandwich configuration, and they shown a mean value for the thickness equal to $t_m = 5.34\,mm$; the standard deviation was found to be equal to $\sigma_t = 0.0652$. The nominal width for the specimens was supposed to be equal to $17.17\,mm$. Also in this case, a certain variability was found

Table 3: Cross-head rate of motion R and deflection D at outer fibers strain equal to 0.05 mm/mm.

	Cross-head rate and deflection according to ASTM D790							
Specimen	1	2	3	4	5	6	7	8
R[mm/min]	2.52	2.47	2.55	2.54	2.56	2.49	2.46	2.52
D[mm]	12.59	12.36	12.76	12.69	12.78	12.43	12.32	12.62
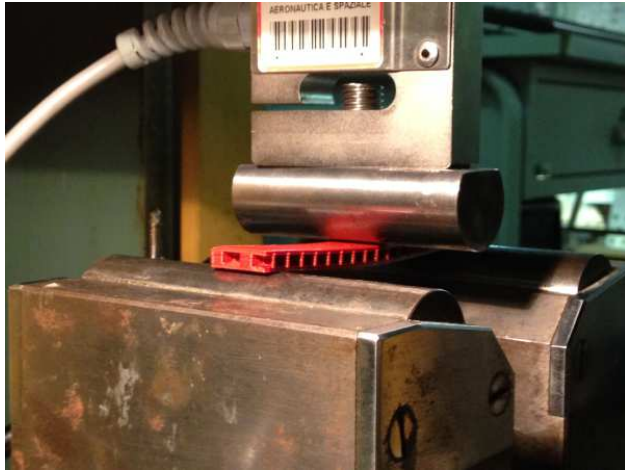
Figure 2: Specimen 1 during the three-point bending test.
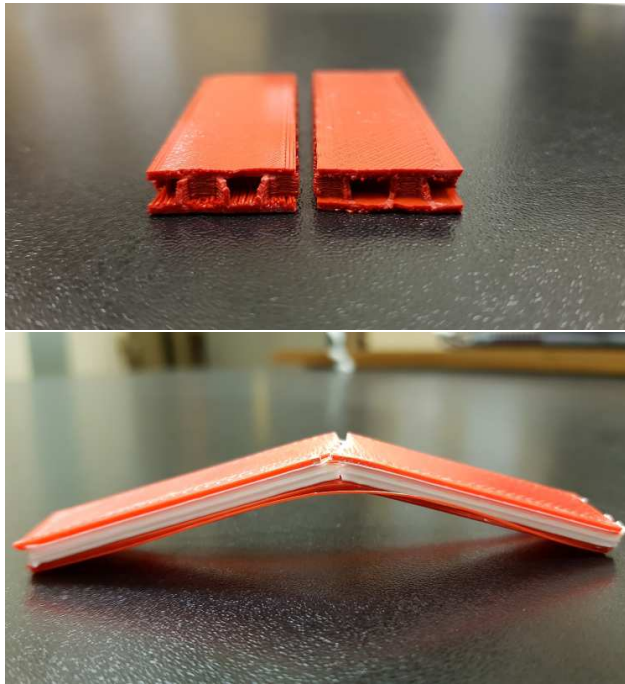
Figure 3: Specimen 1 (on the top) and specimen 6 (on the bottom) after the three-point bending test.

for the first group of 5 specimens. The mean value for this quantity is therefore $w_m = 17.272 mm$ with a standard deviation of $\sigma_w = 0.1779$.

After the evaluation of the geometrical characteristics, it was possible to set-up the experiment. Each test specimen was positioned horizontally in a resting position over two supports. Figure 2 shows the example for the specimen 1 during the test. The load was given by a vertical nose, symmetrically positioned between the two supports, and acting on the upper surface. In accordance with the nomenclature reported in [44], a Type I test was executed in accordance with the procedure A. The deflection of the specimen during the loading stage was measured using the information obtained by the cross-head position. The cross-head motion was set up using a constant strain rate of $0.01 mm/mm/min$ for the outer fiber. The rate of the cross-head motion was calculated as:

$$R = \frac{ZL^2}{6d} . \tag{1}$$

In Eq.(1), Z stands for the straining rate of the outer fiber; it was imposed equal to $0.01 mm/mm/min$. L is the distance between the two supports of the testing machine, it is equal to $90 mm$. d is the thickness of the specimen to be tested. In place of the nominal value, the experimentally measured value was used for each of the eight specimens. R was therefore expressed in [mm/min]. Table 3 shows the cross-head rate of motion for each of the 8 specimens. The procedure made according to this standard is preferable for those materials that break or yield in the outer surface within a strain limit evaluated in 5.0%. An ex-post verification was made and this standard was found to be applicable for all the presented configurations, with exception for the specimen embedding a homogeneous PLA core. As reported in [44], the deflection amplitude which corresponds to a strain in the outer fibers equal to 0.05 mm/mm must be calculated using the following expression:

$$D = \frac{rL^2}{6d} . \tag{2}$$

In Eq.(2), r is the strain of the outer fibers and it was set equal to the reference value. L and d have been described before. The deflection D is given in the last line of Table 3.

Figures 3 and 4 show the specimens 1, 6, 7 and 8 after the test. The family of the first 5 specimens (see the example in Figure 3 for specimen 1) broke with a brittle failure when the maximum tensile stress (in the lower fibers) or

Table 4: Flexural modulus of elasticity and flexural strength for the eight proposed specimens.

Mechanical characteristics								
Specimen	1	2	3	4	5	6	7	8
$E[N/m^2]$	2034	1837	2114	2019	1964	1378	794	969
$\sigma_{max}[N/m^2]$	53.32	43.16	52.28	49.84	44.02	48.60	12.21	8.39
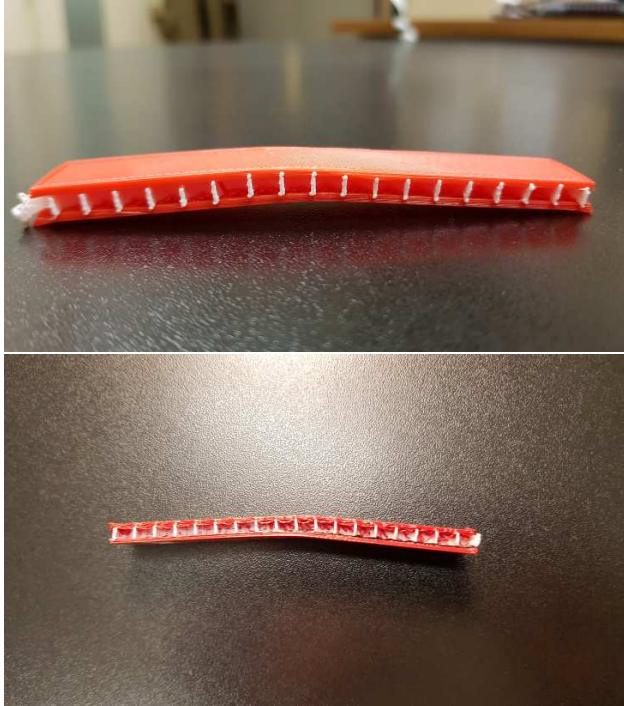
Figure 4: Specimen 7 (on the top) and specimen 8 (on the bottom) after the three-point bending test.

the maximum compressive stress (in the upper fibers) was reached. The same behavior has been shown for specimen 6 embedding a homogeneous PLA core. Specimens 7 and 8 have a different behavior with respect to specimens 1-5 and 6. The failure happened when the delamination between the lower skin (the one which experimented tensile stresses) and the internal core appears. This feature suggested that the failure could have been affected by an inadequate adhesion between the layers.

3 Preliminary bending results and mechanical behavior of sandwich specimens

Figures 5-8 show the raw data trends, giving the deflection of the center of the beam in [mm] versus the applied load in [N]. A preliminary analysis of the proposed curves shows that all the specimens independently by the material and the stacking sequence, experimented an initial linear trend. Furthermore, the end of this behaviour is clearly indicated by an abrupt change in the curve shape which basically coincides with the break of the outer skins. The post-process of the raw experimental data was made using the dictates provided by the reference standard [44]. In order to obtain the typical stress-strain curves, the flexural stress and the flexural strain were calculated. The flexural stress is defined as the maximum stress experimented by the specimen under a certain load. Given the geometry, the boundary conditions and the load configuration, the maximum stress occurred in correspondence to the outer surface (at the midpoint) was calculated as:

$$\sigma_f = \frac{3PL}{2bd^2} \; . \tag{3}$$

In Eq.(3), P is the load at the considered point and it is expressed in [N]. b is the width of the considered specimen. L and d have been already described. The flexural strain is defined as the strain of the outer surface at the midpoint, where its maximum value is reached. It was calculated as:

$$\epsilon_f = \frac{6Dd}{L^2} \; . \tag{4}$$

All the quantities involved in Eq.(4) have been previously defined. Using the definitions given in Eqs. (3) and (4), the following mechanical characteristics of the proposed configurations were calculated.

Flexural Strenght. It is defined as the maximum value of the flexural stress which can be sustained by the specimen.

Modulus of Elasticity. It indicates the material resistance to deformation under stress. From a graphical point of view, it indicates the slope of the stress-strain curve at a certain stress level. As anticipated, all the specimens showed an initial Hookean behavior; in this portion of the graph, the trend of the stress-stain curve is almost linear. The stress level which corresponds to a change in the slope of the curve was identified. Defining as N_s this N-th point, a Matlab tool was implemented to build $N_s - 1$ ranges of values. The N-th range contains all the values included between the first one and $N - 1$ point. A linear regression
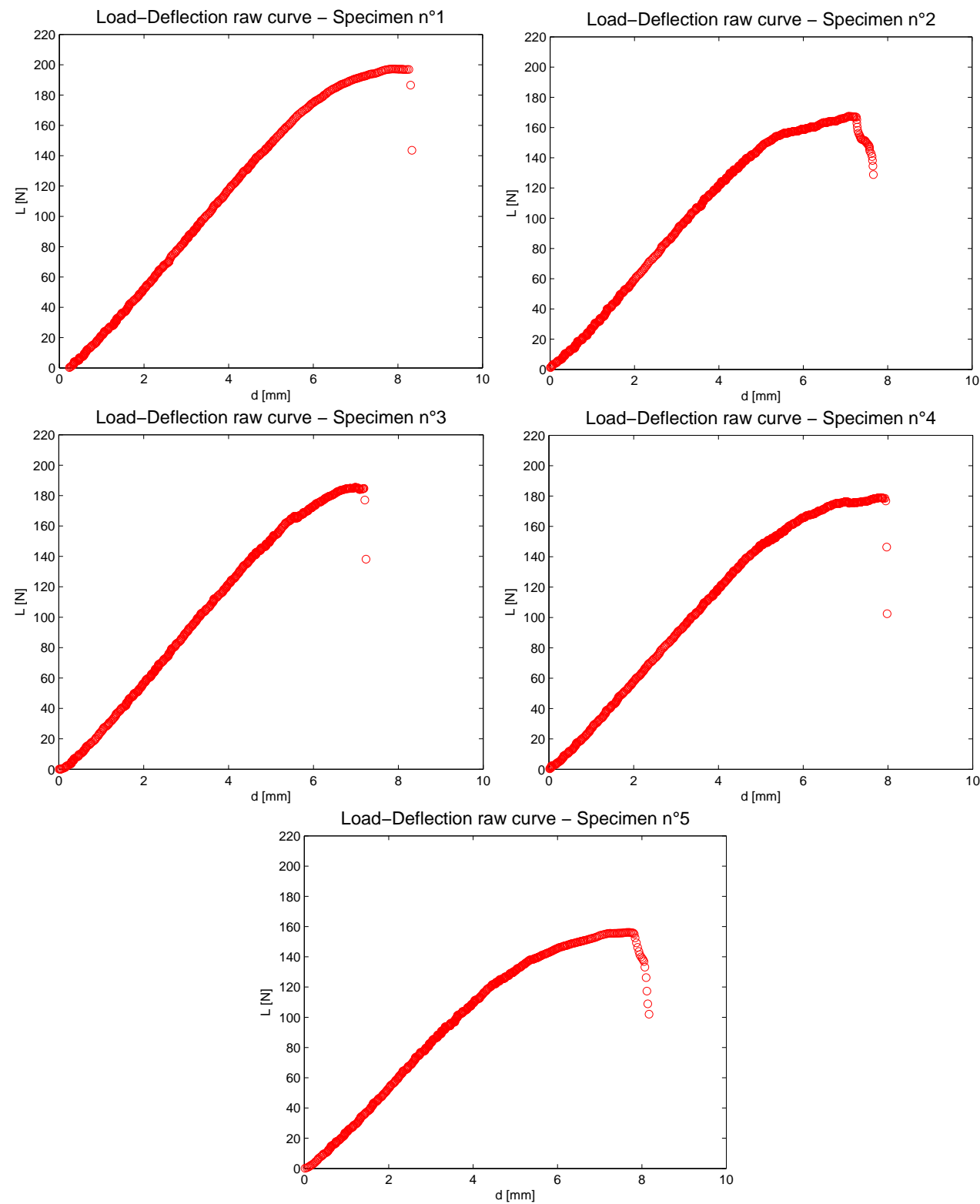
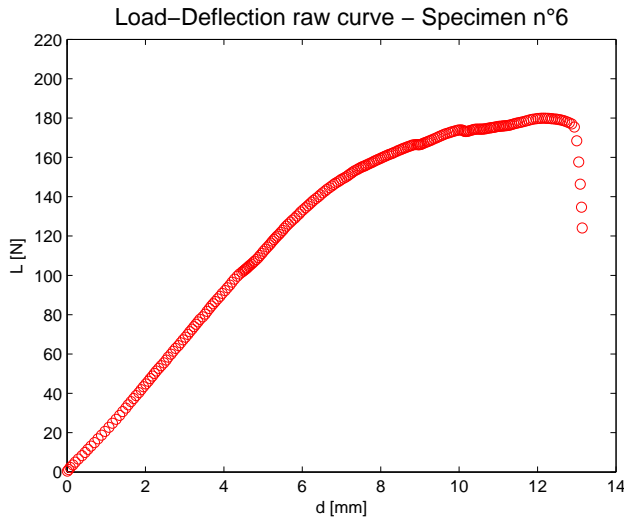**Figure 5:** Raw load-deflection curves for specimens 1-5.

Figure 6: Raw load-deflection curve for specimen 6.
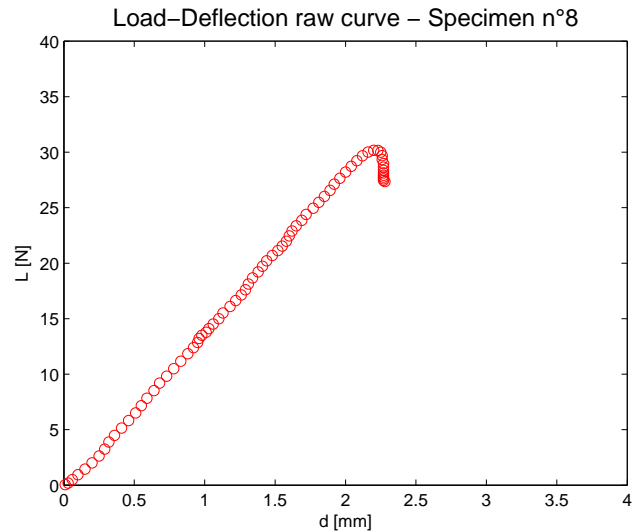

Figure 8: Raw load-deflection curve for specimen 8.
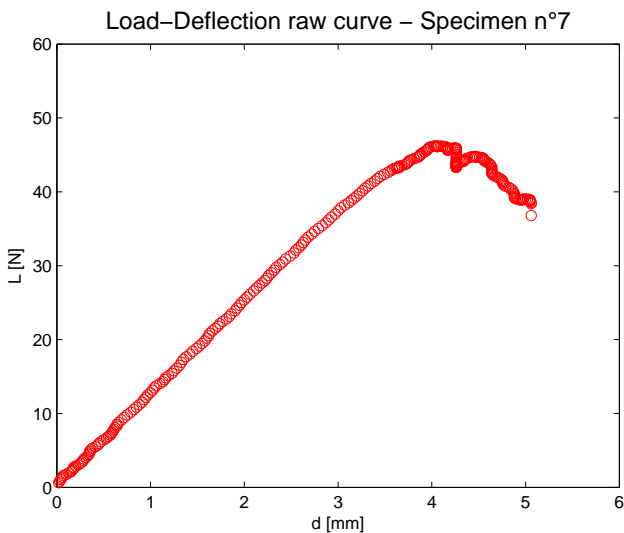

Figure 7: Raw load-deflection curve for specimen 7.

based on each of these ranges was made; the coefficients were, then, averaged.

3.1 Results

The plots of the stress-strain curves for each of the 8 specimens are shown in Figures 9-12. The results in terms of flexural strain and modulus of elasticity are reported in each graph and they are summarized in Table 4. The first 5 specimens for the PLA sandwich structure embedding a honeycomb core and produced via a single extruder are proposed in Figure 9. For this group, a simple statistical analysis is possible. The three remaining sandwich specimen types have been produced as only one element for each type.

Therefore, they are only used to make some preliminary assessments and comparisons. Figure 13 shows the probability plot of the calculated moduli of elasticity for the PLA specimens with honeycomb core produced via a single extruder process. The mean value for the flexural modulus is $1994N/mm^2$, with a standard deviation of $102.7N/mm^2$. A certain variability is present. It is interesting to notice that specimen 2 appeared to be less performing if compared with the other four specimens of the same group. Figure 14 compares these results with those obtained with the other three specimens (one for each remaining type). The specimen with ABS skins and PLA honeycomb core showed the worst performances, with an elastic modulus of only $794N/mm^2$, which is less than half of that for the first configuration. A similar performance was obtained for the specimen with PLA skins and PLA honeycomb core obtained via two different extruders. Its stiffness was evaluated in $969N/mm^2$. Better performances were shown by the specimen with homogeneous PLA core and external ABS skins, $1378N/mm^2$ was the calculated value for the bending stiffness of this specimen type.

The probability plot for the flexural strength of the PLA specimens with skins and honeycomb core printed with the same extruder is presented in Figure 15. An average value of $48.52N/mm^2$ was found, with a standard deviation of $4.69N/mm^2$. Also in this case, a significant variability is present, as the lower assumed value is equal to $43.16N/mm^2$ while the highest one is $53.32N/mm^2$. It is interesting to note that the lowest value was recorded for the specimen 2, which is the same specimen that experimented the lowest modulus of elasticity. The comparison between these results and those for the other three types of
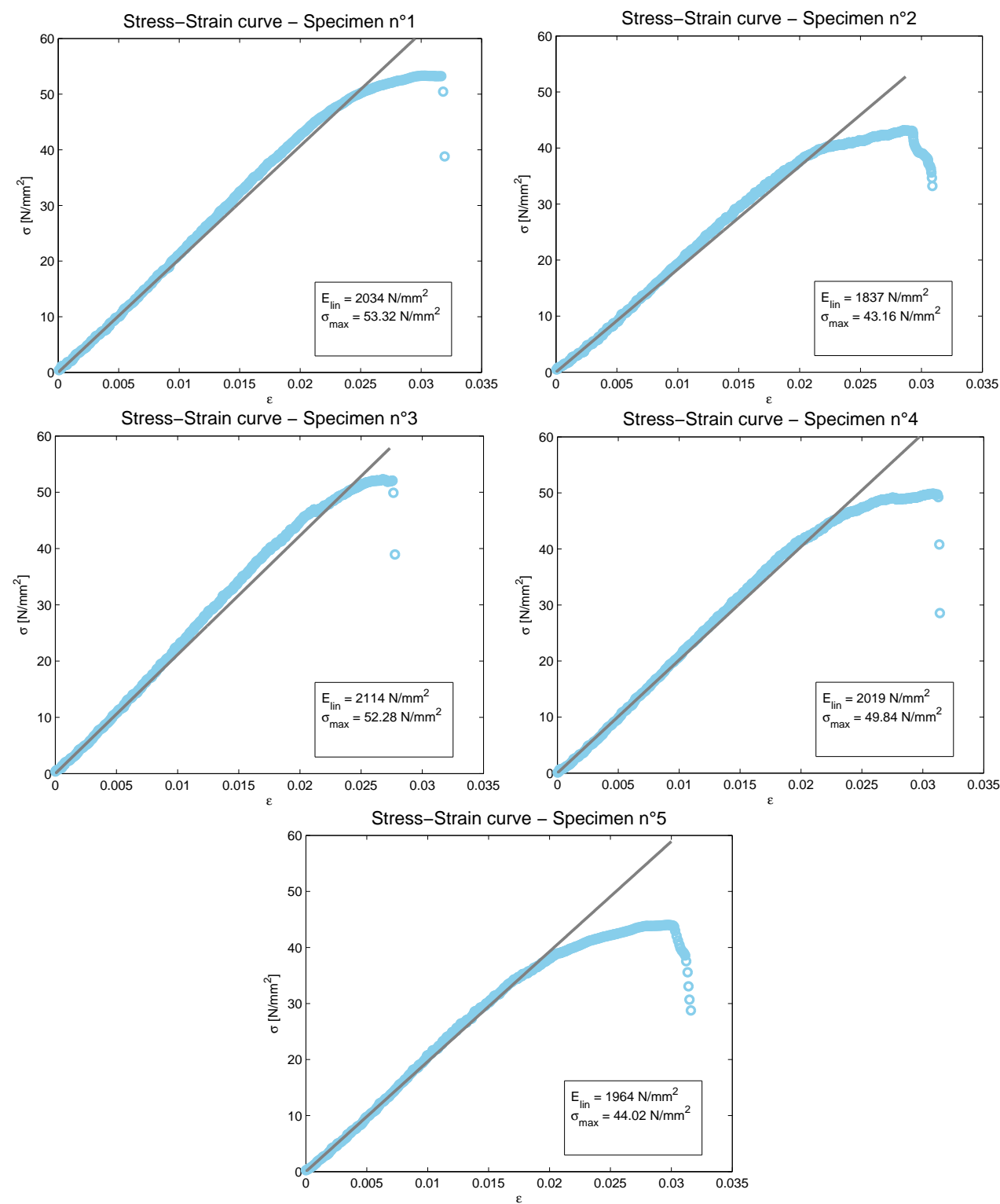
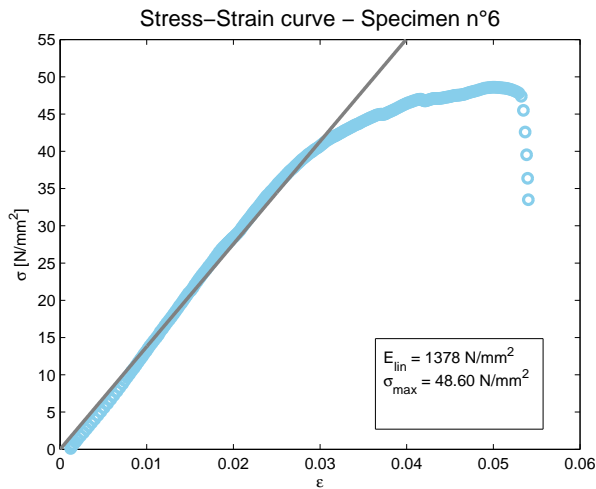**Figure 9:** Stress-strain curves for specimens 1-5.

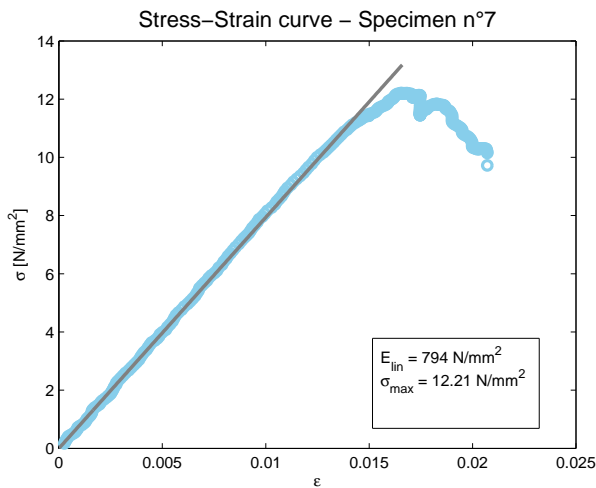**Figure 10:** Stress-strain curve for specimen 6.

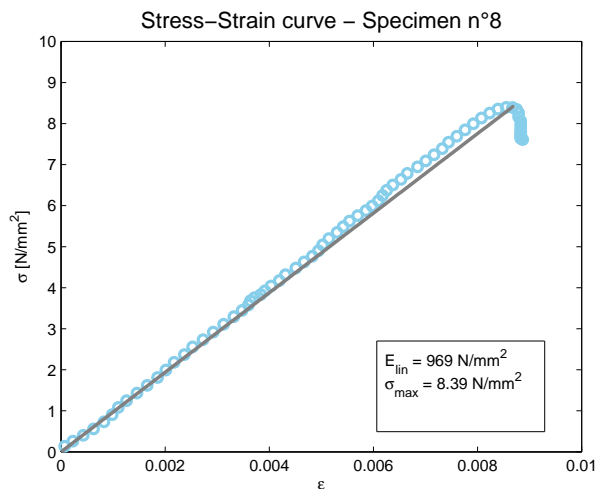**Figure 11:** Stress-strain curve for specimen 7.

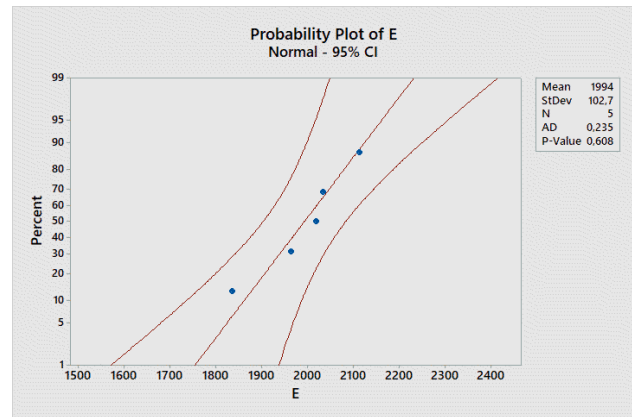**Figure 12:** Stress-strain curve for specimen 8.

Figure 13: Probability plot of the flexural modulus of elasticity $[N/m^2]$ for specimens 1-5.
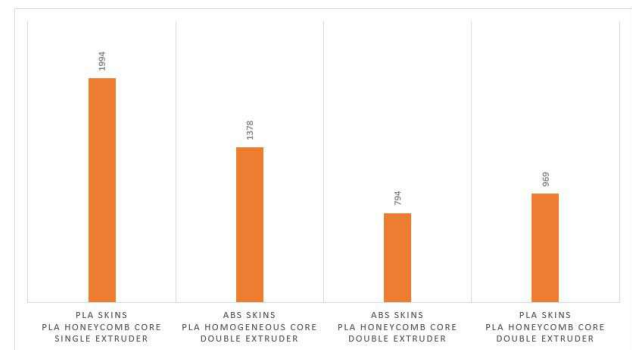

Figure 14: Comparison between the flexural moduli of elasticity $[N/m^2]$ for the four specimen types.
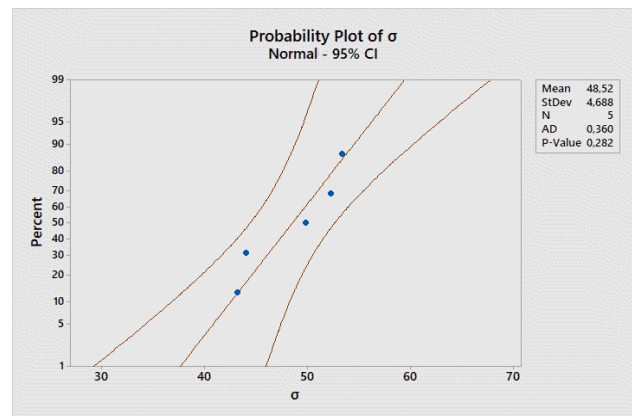

Figure 15: Probability plot of the flexural strength $[N/m^2]$ for specimens 1-5.

specimens is given in Figure 16. The performance proven by the specimen with homogeneous PLA core was comparable with the one shown by the reference configuration investigated in Figure 15: a value of $48.60 N/mm^2$ was measured. The other two specimen types with PLA honeycomb core have lower values which are $12.21 N/mm^2$ and
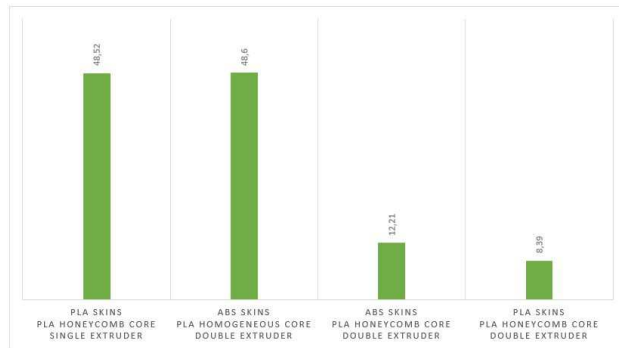
Figure 16: Comparison between the flexural strengths [N/m^2] for the four specimen types.

8.39N/mm^2. The main reason of this bad performance is again the delamination as already explained above.

4 Conclusions and future developments

The paper presented a preliminary evaluation of the flexural properties of sandwich specimens produced with a home desktop 3D printer based on the FDM technology. The main focus was devoted to a single material configuration where both the internal honeycomb core and the external skins are made of PLA via a single extruder. The average values of 1994N/mm^2 for the flexural modulus of elasticity and 48.52N/mm^2 for the flexural strength were found. 5 specimens were used for this configuration. Specimen 2 showed significantly lower performances than the other 4 specimens. During the post-processing of the results, it was assessed that this specimen was tested differently than the other four ones. In fact, the other 4 specimens were tested using the upper surface as surface where the loading nose acted. On the contrary, specimen 2 was placed upside-down. The idea is that the heat generated by the printing floor is responsible of a pre-stress.

The substitution of PLA with ABS for the external skins resulted in lower performances for the modulus of elasticity because of the use of two different extruders. Therefore, a bad adherence between the skins and the core is shown. This effect is related with the interaction between the two different materials (ABS and PLA) and on the subsequent print of the three layers by means of two different extruders. In fact, the specimen with PLA core and skins, separately printed with two different extruders, showed similar performances. An improvement is obtained using a homogeneous PLA core in place of the honeycomb PLA core

when ABS skins are added by means of a second extruder. These features suggest that the bad adhesion between the layers could be linked to both the process and the materials. The idea is that the transition between the first and the second extruder gives an early cooling of the previously printed layer reducing the ability of completely adhering to the second layer. This effect is partially reduced for the homogeneous PLA core because the limit surface between layers is greater. Because of these interesting partial conclusions, further analysis are needed to clarify these indications and to perform a statistically stable behaviour.

References

[1] G.N. Levy, R. Schindel and J.P. Kruth, Rapid manufacturing and rapid tooling with Layer Manufacturing (LM) technologies, state of the art and future perspectives, CIRP Annals, 52, 589-609, 2003.

[2] S. Brischetto, P. Maggiore and C.G. Ferro, Special Issue on "Additive Manufacturing Technologies and Applications", Technologies, 5, 1-2, 2017.

[3] B. Lu, D. Li and X. Tian, Development trends in additive manufacturing and 3D printing, Engineering, 1, 85-89, 2015.

[4] S. Brischetto, A. Ciano and C.G. Ferro, A multipurpose modular drone with adjustable arms produced via the FDM additive manufacturing process, Curved and Layered Structures, 3, 202-213, 2016.

[5] S. Brischetto, A. Ciano and A. Raviola, Patent application for industrial invention, A multipurpose modular drone with adjustable arms, registered on 5th November 2015 with temporary number 102015000069620.

[6] S. Brischetto, Innovative multilayered structures for a new generation of aircraft and spacecraft, Journal of Aeronautics & Aerospace Engineering, 4, 1-2, 2014.

[7] G.D. Goh, S. Agarwala, G.L. Goh, V. Dikshit, S.L. Sing and W.Y. Yeong, Additive manufacturing in unmanned aerial vehicles (UAVs): challenges and potential, Aerospace Science and Technology, 63, 140-151, 2017.

[8] M.K. Agarwala, V.R. Jamalabad, N.A. Langrana, A. Safari, P.J. Whalen and S.C. Danforth, Structural quality of parts processed by fused deposition, Rapid Prototyping Journal, 2, 4-19, 1996.

[9] I.M. Daniel and J.L. Abot, Fabrication, testing and analysis of composite sandwich beams, Composites Science and Technology, 60, 2455-2463, 2000.

[10] A. Russo and B. Zuccarello, Experimental and numerical evaluation of the mechanical behaviour of GFRP sandwich panels, Composite Structures, 81, 575-586, 2007.

[11] C.A. Steeves and N.A. Fleck, Collapse mechanisms of sandwich beams with composite faces and a foam core, loaded in three-point bending. Part I: analytical models and minimum weight design, International Journal of Mechanical Sciences, 46, 561-583, 2004.

[12] J.W. Hutchinson and Z. Suo, Mixed mode cracking in layered materials, Advances in Applied Mechanics, 29, 63-191, 1992.

[13] O. Luzanin, D. Movrin and M. Plancak, Effect of layer thickness, deposition angle, and infill on maximum flexural force in FDM-built specimens, Journal for Technology of Plasticity, 39, 49-58, 2014.

[14] R. Melnikova, A. Ehrmann and K. Finsterbusch, 3D printing of textile-based structures by Fused Deposition Modelling (FDM) with different polymer materials, IOP Conf. Series: Materials Science and Engineering, 2014 Global Conference on Polymer and Composite Materials (PCM 2014), 62, 012018, 2014.

[15] P. Gu and L. Li, Fabrication of biomedical prototypes with locally controlled properties using FDM, CIRP Annals, 51, 181-184, 2002.

[16] A. Pan, Z. Huang, R. Guo and J. Liu, Effect of FDM process on adhesive strength of PolyLactic Acid (PLA) filament, Key Engineering Materials, 667, 181-186, 2016.

[17] P. Minetola, L. Iuliano and G. Marchiandi, Evaluation of the flexural behaviour of 3D printed multimaterial beams, EUPOC 2017 - Polymers and Additive Manufacturing: from fundamentals to applications, Gargnano (BS) - Italy, 21-25 May 2017. p. 34.

[18] S. Kumar and J.-P. Kruth, Composites by rapid prototyping technology, Materials and Design, 31, 850-856, 2010.

[19] L.C. Magalhaes, N. Volpato and M.A. Luersen, Evaluation of stiffness and strength in fused deposition sandwich specimens, Journal of the Brazilian Society of Mechanical Sciences and Engineering, 36, 449-459, 2014.

[20] P. Parandoush and D. Lin, A review on additive manufacturing of polymer-fiber composites, Composite Structures, 182, 36-53, 2017.

[21] J.L. Tan and C.H. Wong, Review of multi-material additive manufacturing, Proceedings of the 2nd International Conference on Progress in Additive Manufacturing (Pro-AM 2016), 294-299, 2016.

[22] O.S. Es-Said, J. Foyos, R. Noorani, M. Mendelson, R. Marlothg and B.A. Pregger, Effect of layer orientation on mechanical properties of rapid prototyped samples, Materials and Manufacturing Processes, 15, 107-122, 2000.

[23] J. Wang, H. Xie, Z. Weng, T. Senthil and L. Wu, A novel approach to improve mechanical properties of parts fabricated by fused deposition modeling, Materials and Design, 105, 152-159, 2016.

[24] L. Bade, P.M. Hackney, I. Shyha and M. Birkett, Investigation into the development of an additive manufacturing technique for the production of fibre composite products, Procedia Engineering, 132, 86-93, 2015.

[25] Z. Quan, A. Wu, M. Keefe, X. Qin, J. Yu, J. Suhr, J.-H. Byun, B.-S. Kim and T.-W. Chou, Additive manufacturing of multidirectional preforms for composites: opportunities and challenges, Materials Today, 18, 503-512, 2015.

[26] R.R. Williams, W.E. Howard and S.M. Martin, Composite sandwich structures with rapid prototyped cores, Rapid Prototyping Journal, 17, 92-97, 2011.

[27] D. Espalin, J.A. Ramirez, F. Medina and R. Wicker, Multi-material, multi-technology FDM: exploring build process variations, Rapid Prototyping Journal, 20, 236-244, 2014.

[28] V. Dikshit, A.P. Nagalingam, Y. Ling Yap, S. Leong Sing, W. Yee Yeong and J. Wei, Crack monitoring and failure investigation on inkjet printed sandwich structures under quasi-static indentation test, Materials and Design, 137, 140-151, 2018.

[29] A. Bagsik, S. Josupeit, V. Schoeppner and E. Klemp, Mechanical analysis of lightweight constructions manufactured with fused deposition modeling, Proceedings of PPS-29. AIP Conference Proceedings, 1593, 696-701, 2014.

[30] T. Li and L. Wang, Bending behavior of sandwich composite structures with tunable 3D-printed core materials, Composite Structures, 175, 46-57, 2017.

[31] F. Riss, J. Schilp and G. Reinhart, Load-dependent optimization of honeycombs for sandwich components - New possibilities by using additive layer manufacturing, Physics Procedia, 56, 327-335, 2014.

[32] L. Yang, O. Harrysson, H. West and D. Cormier, Mechanical properties of 3D re-entrant honeycomb auxetic structures realized via additive manufacturing, International Journal of Solids and Structures, 69-70, 475-490, 2015.

[33] M. Bici, S. Brischetto, F. Campana, C.G. Ferro, C. Seclí, S. Varetti, P. Maggiore and A. Mazza, Development of a multifunctional panel for aerospace use through SLM Additive Manufacturing, 11th CIRP Conference on Intelligent Computation in Manufacturing Engineering, Ischia (Italy), July 2017.

[34] C.G. Ferro, S. Varetti, S. Brischetto and P. Maggiore, Mechanical behaviour of a multifunctional panel for de-icing systems, Mechcomp 3 - 3rd International Conference of Mechanics of Composites, Bologna (Italy), 4-7 July 2017.

[35] C.G. Ferro, A.E.M. Casini, A. Mazza, P. Maggiore and S. Brischetto, A novel design approach for space components: application to a multifunctional panel, 68th International Astronautical Congress (IAC), Adelaide (Australia), 25-29 September 2017.

[36] C.G. Ferro, S. Brischetto, R. Torre and P. Maggiore, Characterization of ABS specimens produced via the 3D printing technology for drone structural components, Curved and Layered Structures, 3, 172-188, 2016.

[37] S. Brischetto, C.G. Ferro, P. Maggiore and R. Torre, Compression tests of ABS specimens for UAV components produced via the FDM technique, Technologies, 5, 1-25, 2017.

[38] S. Brischetto, C.G. Ferro, R. Torre and P. Maggiore, Tensile and compression characterization of 3D printed ABS specimens for UAV applications, 2016 3rd International Conference on Mechanical Properties of Materials (ICMPM 2016), Venice (Italy), 14-17 December 2016.

[39] S. Brischetto, C.G. Ferro, P. Maggiore and R. Torre, Characterization and analysis of homogeneous and sandwich PLA/ABS specimens produced via the FDM printing process for UAV structural elements, Mechcomp 3 - 3rd International Conference of Mechanics of Composites, Bologna (Italy), 4-7 July 2017.

[40] C.G. Ferro, S. Brischetto, P. Maggiore and R. Torre, Multi-material sandwich panel produced with desktop 3D printer, Mechcomp 3 - 3rd International Conference of Mechanics of Composites, Bologna (Italy), 4-7 July 2017.

[41] S. Raut, V. Kumar, S. Jatti, N. K. Khedkar and T.P. Singh, Investigation of the effect of built orientation on mechanical properties and total cost of FDM parts, 3rd International Conference on Materials Processing and Characterisation, Procedia Materials Science, 6, 1625-1630, 2014.

[42] S. Ahn, M. Montero, D. Odell, S. Roundy and P. Wright, Anisotropic material properties of fused deposition modeling ABS, Rapid Prototyping, 8, 248-257, 2002.

[43] D. Croccolo, M. De Agostinis and G. Olmi, Experimental characterization and analytical modelling of the mechanical behaviour of fused deposition processed parts made of ABS-M30, Computational Materials Science, 79, 506-518, 2013.

[44] Standard Test Methods for Flexural Properties of Unreinforced and Reinforced Plastics and Electrical Insulating Materials, Annual Book of ASTM Standards, ASTM International, West Conshohocken, PA, USA, 2017.

[45] Standard Test Method for Flexural Properties of Unreinforced and Reinforced Plastics and Electrical Insulating Materials by Four-Point Bending, Annual Book of ASTM Standards, ASTM International, West Conshohocken, PA, USA, 2017.